Author's reply to Anonymous Referee #2's (RC2) comments on manuscript egusphere-2024-4044

This paper presents a complete list of storm surge events recorded in the Bakar Station, northern Adriatic, in the last 90 years. Each event is analysed using the available data, with good filtering of the sea level signal. The paper is well written and of good scientific quality. I congratulate the authors for their work. I have just some comments (see the PDF for the minor comments):

Dear Reviewer,

Thank you for your comments and the time you dedicated to reviewing our manuscript. Our responses to your comments are provided in blue text below, and the corresponding changes to the manuscript are shown in red text insets.

- The authors define these events as "floods", but this word is more related to the inundation aspect, not to the storm surge aspect;

We replaced the word 'floods' with 'extreme sea levels' in the title and throughout the manuscript, where appropriate.

- The results of each event are well presented and discussed, even if they are a bit too long. On the contrary, the general discussion of all the cases is poor. The authors should analyse a bit more the changes in time of the sea level components, since they are related to climate change issues (e.g., MSL rise, storminess). I suggest adding some more material on this.

To improve readability and navigation, we added individual subsections for each episode listed in Table 2. In response to comments from both reviewers regarding the discussion of all episodes, we have restructured and expanded this section to include more information on climate change. Additionally, we performed further analyses to examine the effects of storminess, msl rise, and other factors on the temporal distribution of the intensity and frequency of extreme episodes, as suggested. Please find a new version of Section 5 at the end of this document.

Minor comments from attached pdf document

Lines 71-73: Wave setup was defined a long time ago, find an older citation. It is important only in some areas, specify.

We identified an earlier reference (Bowen et al., 1968) and specified the types of coastal areas where wave setup is significant (wide, gently sloping coastlines). Since this section (1. Introduction) was overlapping with Section 3.2, we have revised both sections and included the updated versions at the end of this document.

Line 82: Really? They are slow and well predictable.

Reformulated. We understand now that the term "threatening" could suggest unpredictability, which was not what we intended to say.

Line 88: Why? Important or more studied?

The sentence has been revised to reflect that we consider it more important, given its increased contribution to the most recent extreme sea-level events.

Line 102: Why Bakar? Is the TS very long? Explain.

Clarification added. It is the oldest TG in Croatia and SL measured here represent the longest recorded series of a single oceanographic parameter in Croatia.

Line 108: Short it. Section title shortened.

Line 113: Give the web address. We have added the link.

Line 114: What is it? Specified.

Table 1: The end is now? Yes, added.

Line 144: I do not agree on this. This definition is the extreme sea level. Floodings are related to the inundation of the territory. Changed in the title and throughout the manuscript where appropriate.

Line 146: You can simply define greater eq than 90cm.

While that would be simpler, it would not be accurate in our context, as the 99.99th percentile is 89 cm for the specified period.

Lne 163: Introduce that you remove tide to analyse the residual, etc… Done! The whole subsection was rewritten.

Line 168: Detided. Use a different achronym or specify it. We specified it (we are now using 'de-tided SL').

Lines 172-173: Insert some citations. Done!

Lines 179-184: Not clear, rephrase it. Rewritten.

Figure 2: Not clear, rephrase it. Rewritten.

Line 190: Citation. Moved to Introduction with citation added.

Line 193: this paper. Changed.

Line 226: Why don't you start from 1 to 27 with the numeration? It's more logical.

Done! The extreme sea-level episodes are now listed in chronological order (from 1 to 27).

Lin 127: () only in the year. Done!

Line 128: Define the acronym. Done!

Line 2081: This section must be reformulated. Please provide some more figures showing general statistics involving all the cases. How (if) did the components change in time?

We have reorganized and expanded this section to address comments from both reviewers. The revised version is provided at the end of this document (Section 5).

Line 2083: Changed.

Line 2090: This is obviously due to the msl rise. Have you also subsidence in the station? A detrended figure would be more interesting.

The Bakar station is located on a stable ground (Međugorac et al., 2022); therefore, subsidence does not contribute to observed sea-level rise at this site. This is now stated in the paper. Also, we have added 'detrended' extremes (derived from total sea levels with mean sea-level change (T > 5 years) removed) alongside 'regular' extremes (derived from raw total sea levels), and we discuss the resulting temporal distribution in relation to mean sea-level rise, storminess, and other contributing factors. Please see section 5 at the end of this document.

Line 2094: What do you mean as intensity? Maximum wind speed? Maximum sea level or wave height?

We meant maximum sea level. This is now clarified in the text.

Lines 2100-2103: This sentence is a bit misleading. Is the relative weight of the components that changed? Or, does the storminess increase? Or does the msl rise accelerate? Show in a graph.

Additional figures have been included to help explain the increased number of extremes toward the end of the studied period. Please see a revised version of Section 5 included at the end of this document.

Line 1102 - 1103: This is not correlated with the previous sentence. This sentence was removed.

Line 2108: Cite the figures. Done!

Figure 73: The caption is hard to understand. Moreover, you should discuss the changes on time. Where is the msl rise? I don't understand the component f. Is the synoptic/storminess component changing (It seems not)? And the other components?

The terminology we originally used for sea-level components was evidently unclear, as reviewers either suggested changes or expressed confusion about what certain components represented. Therefore, we revised the names of the sea-level components:

(a) The *long-period sea-level component* was renamed to *planetary-scale variability* (representing processes with periods between 10 and 100 days). In the figures, this component is now labeled as *'plan'*.

(b) The *mean sea-level change* component was renamed to *long-term sea-level variability*, (representing processes with periods longer than 100 days). In the figures, this component is now labeled as *'long'*.

To address the issue of temporal variability in these components, as raised by the reviewer, we carried out additional analyses, as described in our previous responses. The updated version of this section, *General properties and temporal distribution of SL extremes*, along with the *Conclusions* section, is included at the end of this document.

Line 2148-2156: This is more an introduction than a discussion of the result. Removed.

----

1 Introduction

The Adriatic Sea is a sub-basin of the Mediterranean Sea, surrounded by mountain ranges, everywhere but at the narrow Otranto gate. It is ~850 km long and ~250 km wide, with depths ranging less than 50 m in the northern shelf to 1250 m in the southern Adriatic Pit (Fig. 1). In late autumn and winter, the Adriatic is exposed to frequent passages of Mediterranean cyclones (we use "cyclones" to refer to "extratropical cyclones"), which cause pronounced mean sea-level pressure gradients and consequently a southeast wind Sirocco over the Adriatic (e.g., Trigo and Davies, 2002; Lionello et al., 2021). Under these conditions, the water accumulates in the basin and forms a storm surge which floods the coast. During these events, the northern Adriatic Sea does not behave coherently, i.e. the induced storm surge has a spatial structure that depends on the bathymetry of the basin and the distribution of atmospheric forcing fields (Međugorac et al., 2018). This ultimately determines whether the sea level (SL) response is stronger along the western or the eastern coastline. Although storm surge is a dominant contributor to inundation in the northern Adriatic, other SL processes can have an influence on the formation of extreme SLs on temporal scales of minutes to decades and on some occasions their role can be decisive (Ferrarin et al., 2021; Lionello et al., 2021; Šepić et al., 2022; Ruić et al., 2023). Here we provide an overview of all processes that contribute to extreme sea levels in the northeastern Adriatic, according to their period, from shorter to longer ones: *high-frequency*

oscillations, *tide*, *synoptic component*, *planetary-scale variability* and *long-term sea-level variability*.

High-frequency oscillations (also referred to as *high-frequency component*) represent sea-level oscillations on timescales of minutes to hours, which in this region are primarily driven by short-period seiches and other long gravity waves. Tide-gauge station Bakar (TG Bakar) is situated in Bakar Bay (Fig. 1), which is part of the wider Kvarner Bay region (Kvarner Bay is an area bounded on the outside by a line connecting Cape Kamenjak and Cape Skala, as indicated by the dashed black line in Fig. 1; Goldberg and Kempni, 1938), with both of these bays known for strong seiches. Oscillations in *high-frequency component* recorded in Bakar Bay are induced by mesoscale or synoptic atmospheric disturbances and controlled by area's topography and bathymetry (Goldberg and Kempni, 1938; Šepić et al., 2007).

The astronomic *tide* is one of the main contributors to both positive and negative SL extremes in the Adriatic, from the northwestern to the entire eastern coast (Šepić et al., 2022). In the Adriatic, it is of mixed type and usually modelled as a sum of seven main components – four semidiurnal (K2, S2, M2, N2) and three diurnal (K1, O1, P1). Semidiurnal spring tides occur near the full moon and new moon, while diurnal neap tides occur near the first and last quarter moons. Its amplitude increases towards the closed northern end of the Adriatic: an average daily range in Bakar Bay is ~60 cm, while in Trieste Bay it reaches its maximum at ~120 cm (Medvedev et al., 2020).

Synoptic component denotes sea-level variations driven by synoptic-scale atmospheric disturbances, on timescales of hours to days, and it includes both the forced response (storm surge described above) and free oscillations of the Adriatic (basin-wide seiches). This component plays the most significant role in the formation of the northern Adriatic extremes (e.g., Pasarić and Orlić, 2001; Međugorac et al., 2018; Ferrarin et al., 2021; Lionello et al., 2021; Šepić et al., 2022). If basin-wide seiches are already present in the basin, they can amplify or attenuate an incoming storm surge, depending on their phase relation. The fundamental Adriatic seiche mode has a period of ~21.2 h (e.g., 21.9 h in Schwab and Rao, 1983; 21.2 h in Cerovečki et al., 1997; 21.2 h in Raicich et al. 1999). It is a longitudinal oscillation of the entire basin with a nodal line at the Strait of Otranto (Fig. 1). Once triggered, usually after a storm surge peak when Sirocco suddenly stops or turns to Bora (northeastern wind, c.f., Grisogono and Belušić, 2009), the seiche decays slowly, with an e-folding time of 3.2±0.5 d (Cerovečki et al., 1997). Its initial amplitude can reach several tens of centimetres, and due to its long duration, the seiche can persist through tidal cycles and potentially enhance or attenuate an extreme episode, depending on its phase relative to other involved processes (Šepić et al., 2022).
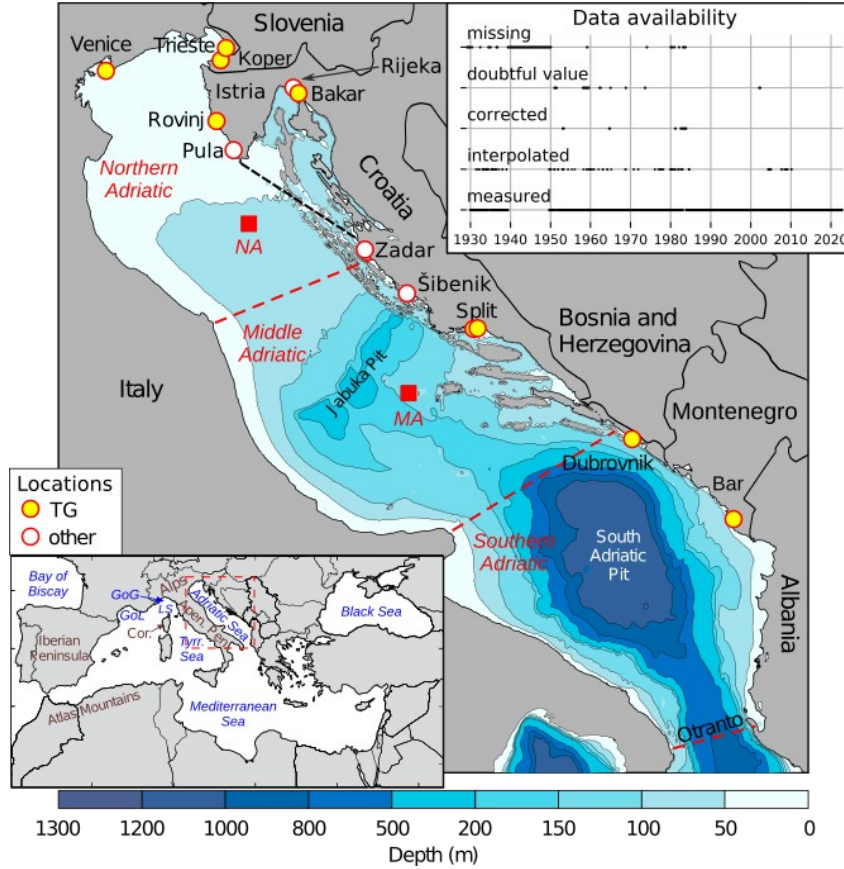
Figure 1: Bathymetry of the Adriatic Sea. Locations of tide-gauge stations with records of at least 60 y (Pérez Gómez et al., 2022) are marked with red-yellow circles. Other major towns along the Croatian Adriatic coast are marked with red-white circles. The subdivision of the Adriatic into sub-basins is marked with red dashed lines and the area of the Kvarner Bay is to the northeast of the black dashed line. The red rectangles mark grid points for which the atmospheric reanalysis series were analysed. The position of the Adriatic in relation to the Mediterranean is shown in the small inset in the lower left corner, and the data availability of TG Bakar time series is shown in the upper right corner. On the Mediterranean map, frequently referenced regions are labelled: Gulf of Genoa (GoG), Gulf of Lion (GoL), Ligurian Sea (LS), Tyrrhenian Sea (Tyrr. Sea), Apennine Peninsula (Apen. Pen.) and Corsica (Cor.).

It should be mentioned that wave setup – defined by Bowen et al. (1968) as "positive changes in mean water level due to the presence of a train of surface waves" – contributes to total SL, particularly in front of wide, gently sloping coasts and during extreme events characterised by high wind waves. This implies that wave setup likely has a greater influence along the exposed western Adriatic coast than along the steep eastern coast, which is protected by a chain of islands. The phenomenon occurs on timescales ranging from hours to days, encompassing both *high-frequency oscillations* and *synoptic component.* Its impact on SL extremes is notable in several Mediterranean regions, including the eastern Adriatic. In front of Bakar Bay, the 99th percentile of wave setup during extreme events is estimated to be between 10 and 20 cm (Toomey et al., 2022; their Fig. 9).

Another important factor contributing to the Adriatic extremes is *planetary-scale variability* (here also referred to as

planetary-scale component), which prevails in periods of 10–100 d. This SL variation is primarily driven by atmospheric planetary waves (i.e., Rossby waves) which are most pronounced in the middle troposphere (~500 hPa) and most energetic during the colder part of the year. Their influence is exerted through changes in surface atmospheric pressure and wind (Pasarić, 2000; Pasarić et al., 2000; Pasarić and Orlić, 2001). Prolonged intervals of raised SL, i.e. positive phases of *planetary-scale variability,* are particularly critical as their amplitudes in Bakar can exceed 30 cm (Pasarić, 2000; Šepić et al., 2022), therefore even not-so-intense cyclones can cause high total SLs during these sustained high SL periods (Međugorac et al., 2021).

Finally, *long-term sea-level variability* (here also referred to as *long-term sea-level component*) acts on timescales longer than 100 d, encompassing seasonal cycle (with periods of 182.5 and 365 d) and other intraannual processes (on periods up to ~1 y), interannual variability (year-to-year changes), (multi)decadal fluctuations, and secular change (here also referred to as linear rate of change or linear trend). This SL variation is influenced by atmospheric and oceanic drivers across a broad region, including the Atlantic Ocean (e.g., Orlić et al., 2018 and sources cited therein; detailed in Appendix A). While its contribution to Adriatic extreme sea levels remains secondary to *synoptic component,* it still represents an important contribution to extremes, reaching up to 28 cm (Međugorac and Pasarić, 2024).

It is assumed that these five processes are independent of each other, as they have sufficiently small amplitudes compared to the depth of the basin so that nonlinear interactions are negligible. The independence of processes has been confirmed for the interactions between the strongest components, tides and storm surges as well as tides and seiches by empirical analyses (e.g., Cerovečki et al., 1997; Marcos et al., 2009) and by numerical experiments (e.g., Lionello et al., 2005; 2006). Therefore, we assume that extreme sea levels in the Adriatic Sea form as a linear superposition of all active processes, and that by studying these processes separately, we can also distinguish between various sources of these processes, and that the intensity and timing of extremes depend on the phases and the amplitudes of all processes involved.

Research of the northern Adriatic SL extremes has mostly been focused on extremes hitting Venice. A comprehensive catalogue of extreme SLs that occurred in Venice between 787 and 1867 was compiled by Enzi and Camuffo (1995). In the 20th and 21st centuries, several northern Adriatic floods have been the subject of numerical modelling and data analysis efforts, which have examined various aspects of these floods, such as events' predictability, meteorological and oceanographic drivers, and the interplay of contributing processes. Still, much of the detailed research has focused on events that severely impacted Venice (e.g., floods of 4 November 1966 and 12 November 2019). The events that were more pronounced along the eastern Adriatic coast (e.g., flood of 1 November 2012; Međugorac et al., 2018) remain less studied in the literature.

The aim of this paper is fourfold: (i) to compile a list of episodes with the highest sea levels recorded at the Croatia's oldest TG station, Bakar, during the period 1929–2022, (ii) to perform a process-oriented analysis of the episodes (examining the contribution of each SL component, along with the synoptic-scale, planetary-scale and climatological context of the episodes), (iii) to summarise the impacts of these events on people's lives and on the natural and built environment along the Croatian coast, and (iv) to review the relevant studies that have addressed

these flooding events in the past. The paper is organised as follows. After the introductory section (Sect. 1), Sect. 2 provides details on the sea-level, meteorological, and archival data used, as well as past studies. used. The methodology and spectral analysis is described in Sect. 3. Section 4 provides a detailed analysis of the most intense floods observed in the northern Adriatic. Section 5 summarises and concludes the paper.Sect. 3 details the methodology, including the spectral analysis and decomposition of the sea-level and atmospheric time series. Sect. 4 provides a comprehensive analysis of the identified extreme episodes. Sect. 5 summarises and discusses the results, and Sect. 6 concludes the paper with the key findings.

3 Methodology

3.2 Decomposition of sea-level and meteorological series

Figure 2 shows the power spectrum of the Bakar SL record, with vertical lines marking the cut-off periods used to separate the total signal into five frequency bands corresponding to the defined components. In our analysis we filter the SL time series into the following five components: (i) *high-frequency oscillations*, (ii) *tide*, (iii) *synoptic component*, (iv) *planetary-scale variability*, and (v) *long-term sea-level variability*. The definition of these components are based on known sea-level drivers, spectral properties and established methodologies (e.g., Šepić et al., 2022).

We first isolated *tide* using harmonic analysis and synthesis. Specifically, we applied MATLAB T_tide toolbox (Pawlowicz et al., 2002) year by year to hourly series. In each yearly subset, *tide* was modelled as the sum of the seven constituents (K1, O1, P1, K2, S2, M2, N2), which are known to capture the majority of the tidal signal in the Adriatic Sea (Janeković and Kuzmić, 2005). Tidal constituents are visible in Fig. 2 as sharp peaks, which are strongest at periods of ~12 and ~24 h, but also visible at shorter (~4.1 h, ~4.9 h, ~6.1 h, and ~8.2 h) and longer (~13.6 d) periods. Although obvious in Fig. 2, longer and shorter constituents were not explicitly included since they have a minor impact on the tidal signal. Šepić et al. (2022) found that the mean absolute difference between tides estimated using all significant harmonics (43 components) and those using only the seven dominant harmonics was 2.48 cm in Bakar (estimated for period 1956–2020). Once *tide* was estimated and removed from the observed SLs, the non-tidal residual (de-tided SL) was further decomposed using filtering methods.

The de-tided SL series were subsequently split into the four non-tidal components by successive digital filtering, proceeding from the longest-period to the shortest. We applied low-pass filters based on Kaiser windows, with half-power points at 100 d, 10 d and 9h. The 100 d and 10 d limits follow established methodologies, while 9 h limit was selected as it corresponds to a minimum in the SL spectrum (Fig. 2). Although the SL spectrum in the low-frequency range is rather monotonic, imposing these divisions is useful because different physical forcing mechanisms dominate on different timescales (e.g., Pugh and Thompson, 1986; Pasarić and Orlić, 2001).

High-frequency component covers periods 2 h < T < 9 h. In our data, it notably includes the Kvarner Bay seiche (broad peak at ~6 h) and the second higher harmonic of the Adriatic-wide seiche (broad peak at ~7.3 h) (Goldberg

and Kempni, 1938; Ruić et al., 2023). To our knowledge, the origin of the increased energy at a period of ~3.2 h is unclear; the peak was reported but not explained by (Šepić et al., 2022). It should be noted that tidal oscillations at periods of ~8.2 h and shorter are also contained in this component.

Synoptic component covers periods 9 h < T < 10 d. It includes storm surges and two longest modes of the Adriatic-wide seiche. The fundamental mode is visible as a broad peak at ~21.2 h and the first higher harmonic as a peak at ~10.8 h (Fig. 2). For each episode, we assessed whether the fundamental basin-wide seiche was present and potentially contributing to *synoptic component.* This was done by visually inspecting the de-tided SL series in search for clearly distinguishable oscillations with 21.2-h period. If such oscillations were observed within up to three days prior to the extreme event, we assumed that the seiche was also active during the episode itself. This is a semi-empirical approach, previously applied in similar studies (Međugorac et al., 2015; Šepić et al., 2022). In this paper, we use it solely to identify the presence of the basin-wide seiche – not to quantify its contribution to SL extremes.
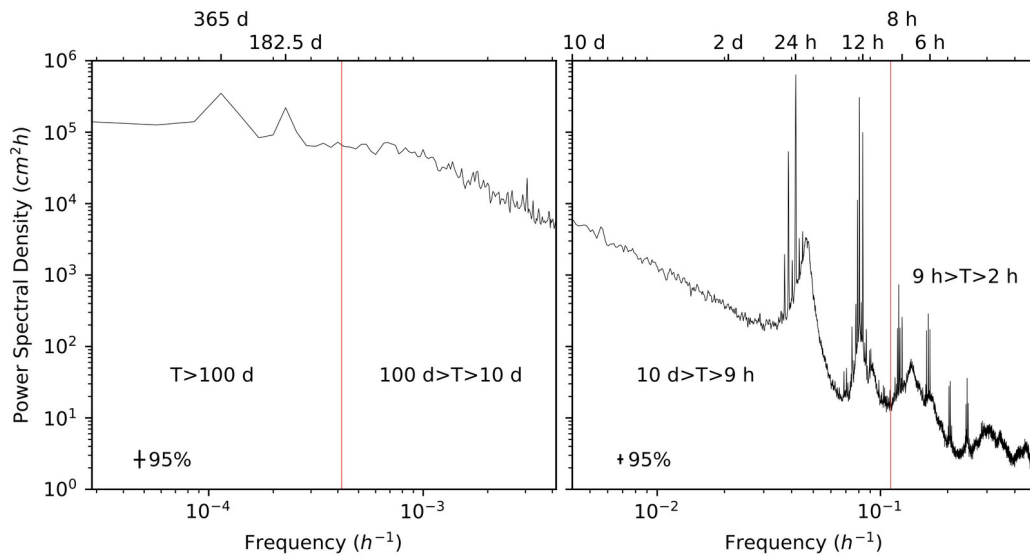
Figure 2: Power spectral densities of total SL measured at TG Bakar (1950–2022), shown for periods longer than 10 d (left) and shorter than 10 d (right). Spectra were computed using Hamming windows with 50% overlap: 4 y windows for the left panel and 1 y windows for the right. Red vertical lines indicate a period of 100 d (left) and 9 h (right). The 95% confidence intervals are indicated. Vertical lines (red and subplot edges) mark boundaries between different sea-level processes.

Planetary-scale component covers periods 10 d < T < 100 d and it is primarily a response of SL to atmospheric Rossby waves. In our data, it also includes a longer-period tidal constituent, visible as a spectral line at ~13.6 d (Fig. 2).

Long-term sea-level variability encompasses processes acting over periods 100 d < T. In this paper, we examined this component in terms of three subprocesses, separated using filters with Kaiser windows: (i) intraannual variability (100 d < T < 15 m), which includes the mean seasonal cycle and its anomalies; (ii) interannual variability (15 m < T < 5 y); and (iii) mean sea-level change (5 y < T), which includes (multi)decadal variations and the secular trend. The intraannual variability was considered instead of the mean seasonal cycle (which is typically derived from a stationary model with fixed amplitude and phase) because the seasonal cycle in the Mediterranean shows

significant interannual variability (e.g., Pérez-Gómez et al., 2021). As a result, using the mean seasonal cycle would not accurately reflect year-to-year changes. Additionally, the upper boundary of 15 months was chosen to avoid splitting the annual process between intraannual and interannual variability.

Figures 3–72 show the five sea-level processes, their contributions to the maxima, and the associated meteorological conditions on synoptic and planetary scales for each episode. Figure 73 presents *long-term sea-level variability*, decomposed into the three aforementioned subprocesses.

Given the high concentration of extreme episodes at the end of the studied period (seven episodes since 2018), we note that for these episodes additional attention should be given to reliability of *long-term sea-level variability*, especially in relation to mean sea-level change (5 y < T). Filtering can heavily affect the edges of time series. To check whether this is an issue for our problem, we compared mean sea-level change calculated first for a full interval (1929–2022; black line in Fig. 73b) and then for a shorter interval (1957–1992; red line in Fig. 73b), and paid special attention to differences between these two series at the edges of the shorter series (1957–1962; 1987–1992). In this way we get an idea about the length of the unreliable marginal period. From Fig. 73b it is evident that mean sea-level change is significantly affected by boundary values, especially in situations when sea level is anomalously high or low, as was the case in 1992 (anomalously low).

To analyse atmospheric forcing on a planetary scale and the corresponding SL response (*planetary-scale component*), we compared low-pass series of MSLP, Z500 and **W10** (filtered with a 10-d cut-off frequency) with joint *planetary-scale* and *long-term sea-level* components. While planetary atmospheric forcing acts over periods 10 d < T < 100 d and thus presumably affects only *planetary-scale component* (10 d < T < 100 d) we use the low-pass filtered series (and not the band-pass ones) because at periods longer than 100 d both atmospheric and SL series show minimal variations over the time frames presented in figures (approximately one month), i.e., series at periods longer than 100 d effectively act as mean values. We focus on MSLP, Z500 and **W10** because, during the colder part of the year (over periods 10 d < T < 100 d), the atmosphere exhibits quasi-barotropic behaviour. This allows disturbances in the middle troposphere (500 hPa) to be reflected at the surface (MSLP and accompanying **W10**), making Z500 a reliable indicator of planetary-scale surface meteorological conditions. In this paper, both in the text and figures, these low-pass series are labelled as MSLP (lp), Z500 (lp), and for sea level, as plan + long.

5 General properties and temporal distribution of SL extremes

This paper analyses the contribution of five sea-level processes to 27 extreme episodes recorded at TG station Bakar, identifying key factors influencing these extremes (Fig. 72). During northern Adriatic episodes, most components were generally in a positive phase, except for *high-frequency oscillations* and *tide* in a few cases, which is consistent with the expectation that extreme sea levels occur when multiple processes constructively overlap. Among the contributors, *high-frequency oscillations* had the least impact, *synoptic component* often played a major role, and other components typically made smaller contributions to the total SL maxima. Towards the end of the studied period (from 2008 onward), the contribution of *synoptic component* became less pronounced compared to

earlier years, while the contributions from *planetary-scale* and *long-term* components increased. Regarding *long-term sea-level component* (Fig. 73), the largest contribution clearly comes from intraannual variability – which includes the mean seasonal cycle and its anomalies (Fig. 73d) – while interannual variations contribute the least (Fig. 73c). The contribution from mean sea-level change (5 y < T) has been positive since the 1996 episode (ID 15), ranging from 2.6 to 8 cm (Fig. 73b).
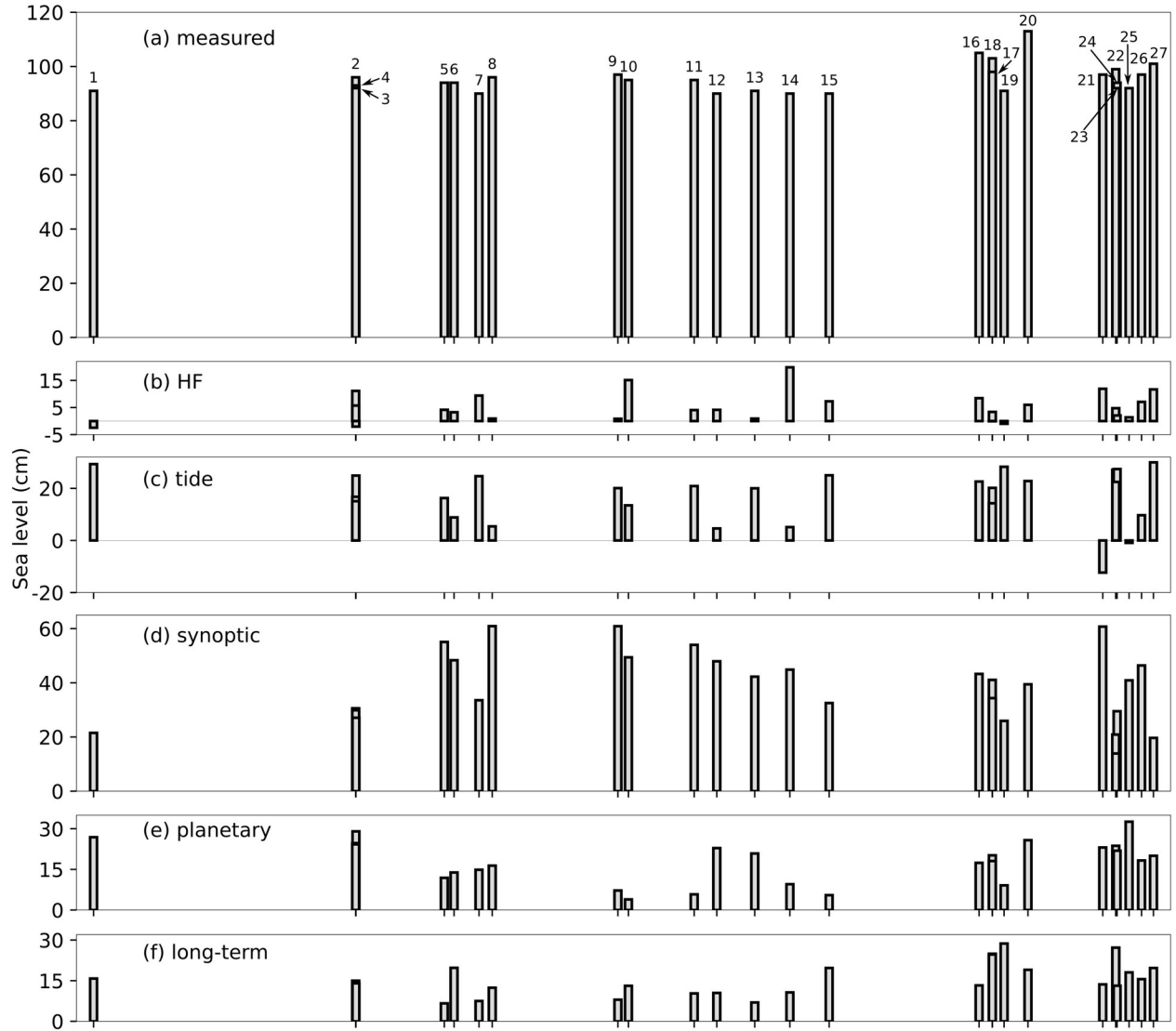
Figure 72: (a) Temporal distribution of total SL maxima observed in Bakar during the 27 extreme SL episodes (marked with their ID numbers from Table 2). Contributions of SL components to observed maxima: (b) *high-frequency oscillations* (2 h < T < 9 h), (c) *tide*, (d) *synoptic component* (9 h < T < 10 d), (e) *planetary-scale component*, (10 d < T < 100 d), and (f) *long-term sea-level variability* (100 d < T).
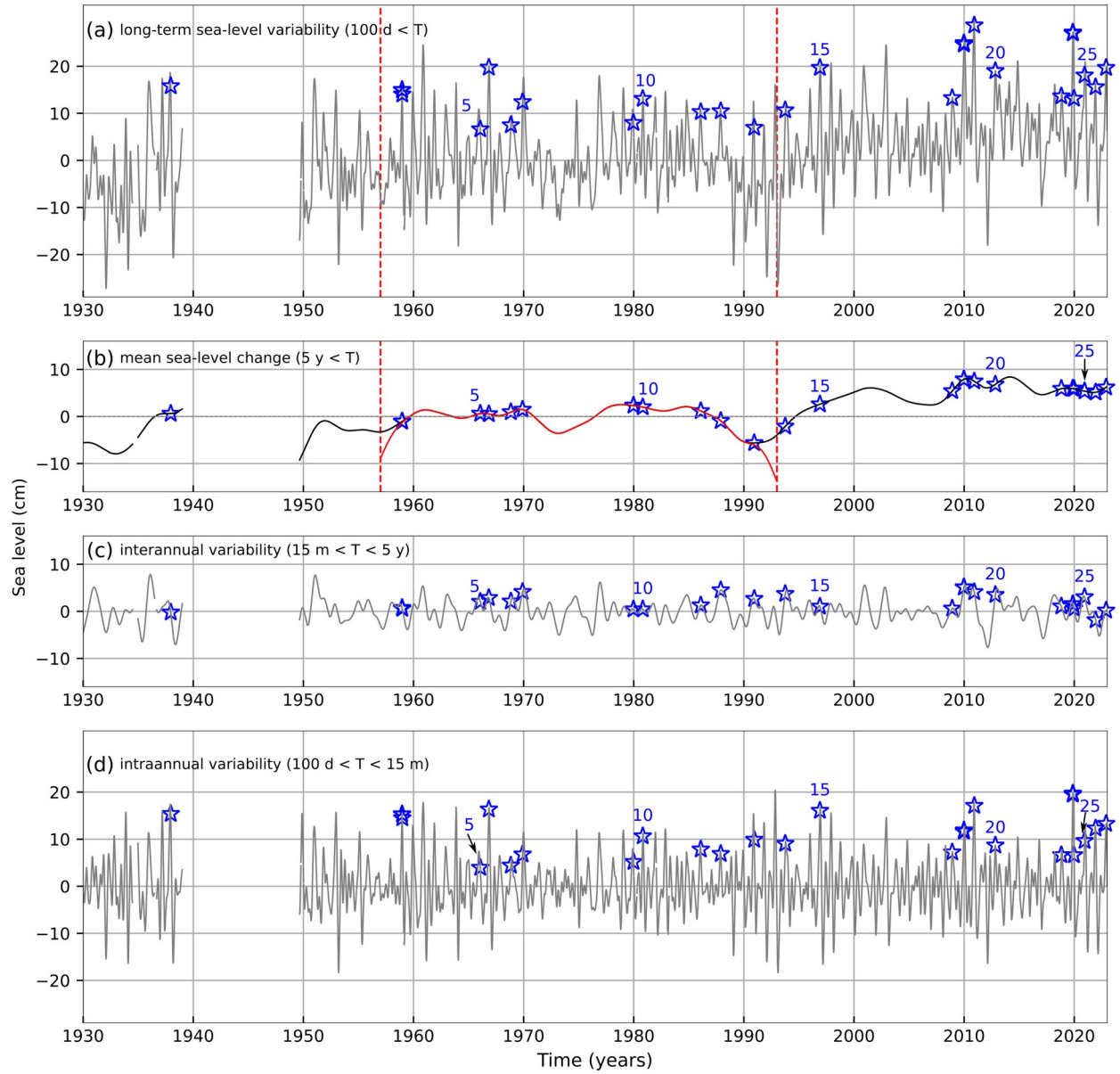
Figure 73: (a) *Long-term sea-level component* representing SL variability at periods longer than 100 d. Red vertical lines indicate the time interval over which mean sea-level change (shown as the red line in panel (b)) was calculated. (b) Mean sea-level change obtained by low-pass filtering SL with a cutoff at a period of 5 y, shown for the 1929–2022 interval (black) and the 1957–1992 interval (red). (c) Interannual variability obtained by band-pass filtering SL at periods between 15 m and 5 y. (d) Intraannual variability, which includes the mean seasonal cycle and its anomalies, representing variations of SL at periods from 100 d to 15 m. Blue stars indicate extracted extreme episodes, with every fifth episode labelled by its ID from Table 2.

Although these conclusions are generally true, each episode is the result of a unique combination of factors. For

example, during the 2 October 1993 episode (Fig. 38), *high-frequency oscillations* – which are typically weak – made a significant contribution. Although still smaller than *synoptic component*, the contribution from *high-frequency oscillations* surpassed the other three components due to the presence of a Kvarner Bay seiche (T~6 h) that peaked simultaneously with the total SL maximum. Similarly, during the 24 December 1958 and 8 December 2020 episodes (Figs. 8 and 65), *planetary-scale component* was strong, comparable to *synoptic component*. This preconditioning resulted from a gradual MSLP (lp) drop, but more importantly from prolonged winds (10 d < T < 100 d) blowing from the south at speeds of up to 7 m/s for a week (2020) or two (1958).

The analysis also underlined the role of pre-existing seiches in extreme SL events. On 10 occasions, a pre-existing seiche was present during an episode and positively overlapped with the newly induced storm surge. Particularly notable events occurred on 18 December 1958 and 23 December 2019, when oscillations triggered a day earlier significantly amplified the subsequent flooding. Despite weak direct forcing during the total SL maxima (Figs. 6, 7d, 60), the total SL exceeded the threshold due to the constructive overlap of the seiche with the tidal daily maxima.

From Fig. 72, it is clear that the largest SL responses to synoptic forcing occurred during extremes in 1966, 1969, 1979, and 2018 (IDs 5, 8, 9 and 21). These episodes, except the 1966, were unaffected by pre-existing seiches (Table 2, Figs. 11, 20, 23, 56), meaning they were primarily driven by storm surges. Most of these episodes were particularly pronounced along the northwestern coast (in front of Venice Lagoon), which likely explains why they have been extensively studied in the scientific literature. The most studied episodes include those on 4 November 1966, 22 December 1979, 1 December 2008, 29 October 2018, and 13 and 15 November 2019.

Another insight into the varied roles of SL processes in extreme events comes from a comparison of episodes in 2019. Specifically, three events occurred roughly 40 days apart, but the contribution from *long-term sea-level component* was rather different. On 13 and 15 November 2019 (IDs 22 and 23, Fig. 59), the contribution was 27 cm (Fig. A1), whereas on 23 December 2019 (ID 24, Fig. 62), it was 13 cm (Fig. A1). This difference was due to intraannual variability, which had a particularly pronounced amplitude that year, leading to significantly different contributions even between episodes just 40 days apart.

The analysis of meteorological conditions showed that most extreme episodes were associated with cyclones approaching from the west, often forming in the western Mediterranean (e.g., the Gulf of Lion, the Ligurian Sea, or further west) or the Gulf of Genoa. These cyclones typically deepened over the Gulf of Genoa before moving eastward across the northern Adriatic. In some cases, the cyclones originated in the Atlantic or western Europe, then travelled to the western Mediterranean before heading towards the northern Adriatic (e.g., 24 November 1987, 10 December 1990, 2 October 1993). In several cases, cyclones followed atypical trajectories. Two notable examples are the episodes of 22 December 1979 and 13 November 2019. In 1979, a cyclone formed in the lee of the Atlas Mountains, moved northeast across Corsica, and then continued northward without crossing the Adriatic (Fig. 22). In 2019, a cyclone originating in the western Mediterranean crossed the Tyrrhenian Sea and entered the Adriatic farther south than usual (Fig. 58ab), generating southerly winds with hurricane gusts over the southern and middle Adriatic (Sect. 4.19.1). Additionally, two other cases stand out because the MSLP gradients over the Adriatic were

not caused by Mediterranean cyclones crossing the Adriatic but instead resulted from much larger MSLP distributions. On 25 December 2009, a significant MSLP gradient across Europe was driven by an anticyclone in eastern Europe and two cyclones in the west – one over the Bay of Biscay and another over northern Italy (Fig. 46c). Similarly, on 17 and 18 December 1958, no cyclones crossed the Adriatic. Instead, the MSLP gradient, and consequently Sirocco winds, were generated by an upper-level trough spanning almost all of Europe and a ridge penetrating from northwest Africa to the eastern Mediterranean. At lower levels, this setup supported cyclonic activity over the Atlantic (Fig. 7ab) and an increase in MSLP in the east. The cyclones were usually accompanied by precipitation, which was often more intense in the northern Adriatic than in the middle and southern Adriatic and frequently exceeded 30 mm in 24 h.

The temporal distribution of the episodes (Fig. 74) reveals that they do not occur uniformly over time, with a notable increase in frequency towards the end of the studied period. Since 2018, at least one episode has occurred each year. In some years, multiple episodes were observed, such as December 1958 (three episodes), January and November 1966 (two episodes), December 2009 (two episodes), and November and December 2019 (three episodes). However, Fig. 74 indicates that the maximum SL of episodes has not increased over time. The highest hourly SL at TG Bakar was recorded on 1 November 2012. Seasonally, these episodes occur in the colder months, from October to February, especially in November and December.
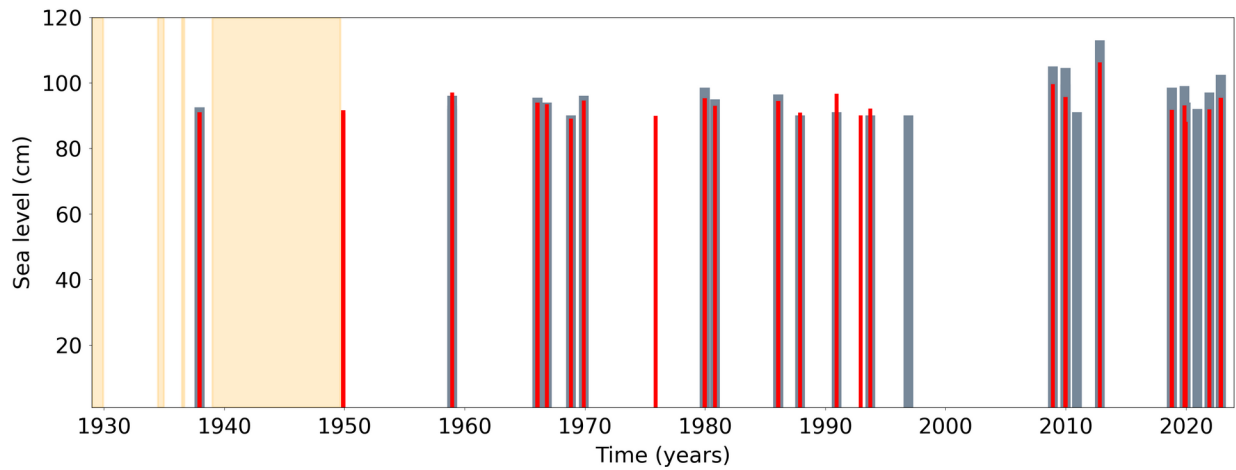
Figure 74: Temporal distribution of extreme SL episodes in the northern Adriatic from 1929 to 2022. Grey bars show the maximum SL recorded at TG Bakar during 27 extreme episodes identified from the total SL series (listed in Table 2). Red bars indicate the maximum SL during episodes extracted from the SL series from which mean sea-level change (5 y < T) was removed (using 99.99th percentile threshold to extract extremes from that series). Orange areas denote periods with data gaps exceeding 30 days.

To explain the higher number of extreme episodes towards the end of the study period, we analysed 'detrended' extremes using the same method as for regular extremes (Section 3.1), but with the mean sea-level change, including

(multi)decadal changes and linear trend, removed from the SL data. It is important to note that the TG Bakar station is located on stable ground, with no evidence of subsidence in its entire operating history (Međugorac et al., 2022); therefore, the observed mean sea-level change at this site reflects only SL change. The temporal distribution of 'detrended' extremes (red bars in Fig. 74) closely mirrors that of the regular extremes (grey bars), with both showing a tendency to cluster, especially in the second half of the period. The sea level recorded on 1 November 2012 remains the highest. Notably, the frequency of episodes remains high towards the end of the period: since 2008, only three (out of twelve) episodes are missing from the 'detrended' set (3 December 2010, 15 November 2019, and 8 December 2020). This indicates that mean sea-level change (which includes (multi)decadal variations and secular trend) is not the main driver of the recent increase in extreme events.

The reasons for this behaviour can be further explored by examining the temporal distribution of the intensity (maximum SL height) and frequency of episodes from other components. To that end, we extracted episodes of extreme *synoptic component* and *planetary-scale variability*, using the same approach as for SL extremes (Sect. 3.1), and applying thresholds selected to yield a similar number of episodes: 51 cm for *synoptic component* and 27 cm for *planetary-scale variability* (Fig. 75). Evidently, the height of synoptic extremes did not increase over time (blue triangles in Fig. 75), although their occurrence remained frequent towards the end of the studied period. A similar conclusion can be drawn for *planetary-scale variability* (green rectangles in Fig. 75), although its clustering is less pronounced. Extreme SLs typically occurred during intervals when at least one of the other components – most often *synoptic component* – was active. However, extreme SLs were not necessarily a direct result of synoptic extremes: in only nine cases could a clear connection be made (circles with blue edges in Fig. 75). Both *synoptic component* and *planetary-scale variability* exhibited periods of reduced activity – in the first half of 1950s, throughout the 1970s, and during a prolonged interval from the 1990s to shortly after 2010. Despite the scarcity of extremes in these components during the last interval, a significant number of extreme SLs still occurred. These events may be explained by other contributing factors: substantial input from *high-frequency oscillations* (ID 14, Fig. 38), large contributions from *long-term sea-level component* (IDs 17, 18, 19; Figs. 47 and 50), or a finely tuned overlap of multiple milder processes (IDs 15, 16, 20; Figs. 41, 44, and 53).

Considering all of the above, we conclude that the frequent occurrences of extreme SLs in the past decade (IDs 20–27) were primarily driven by the increased number of extreme episodes in *synoptic* and *planetary-scale* components.
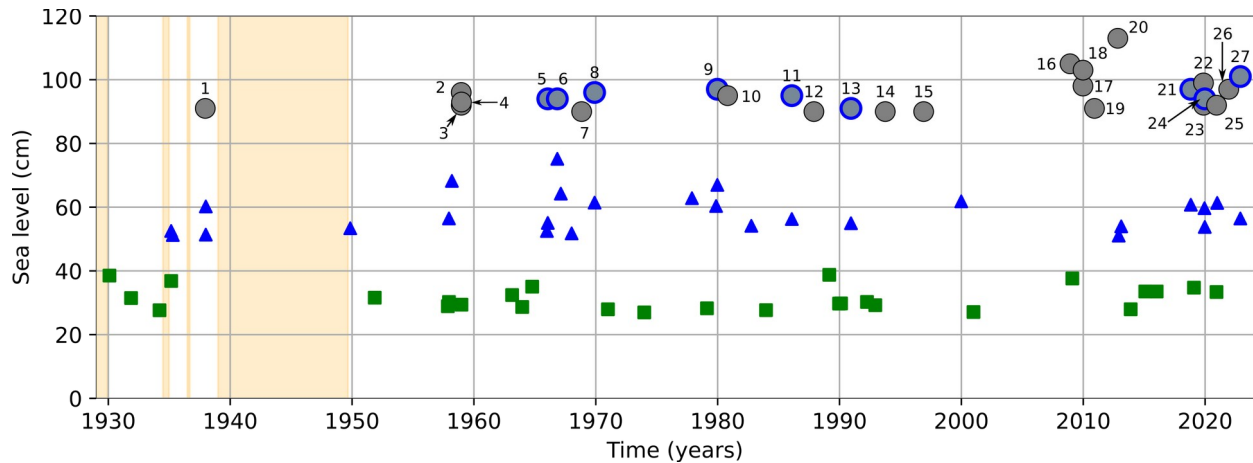
Figure 75: Temporal distribution of: extreme episodes of total SL (grey circles), extreme episodes of *synoptic component* (blue triangles), and extreme episodes of *planetary-scale variability* (green rectangles). Extremes of total SL that coincide with extremes of *synoptic component* are marked with blue edges. Orange shaded areas denote periods with data gaps exceeding 30 days.

6 Conclusions

In this paper, we analysed 27 extreme SL episodes defined as occasions when the hourly SL measured at TG Bakar (northern Adriatic) exceeded 89 cm (99.99th percentile threshold). The study included an empirical analysis of the meteorological background and sea-level evolution for each episode, along with a review of previous scientific literature examining these episodes and a review of daily newspaper and online sources describing their impacts on the natural and built environment along the Croatian coastline.

The analysis revealed several key findings:

- The frequency of extreme sea-level episodes has increased since 2008, although the maximum sea-level values have not exhibited a consistent upward trend. The primary reason for the increase is the frequent occurrence of extreme events driven by synoptic and planetary-scale processes, with mean sea-level change playing a secondary role.

- All episodes occurred between October and February, particularly in November and December.

- The combination of multiple SL components – especially *synoptic component* – drives the most severe episodes, although *planetary-scale* and *long-term* contributions have become more significant in recent years.

- Pre-existing seiches amplified SL maxima in 10 cases.

- While most cyclones associated with these episodes followed typical paths, originating in the western Mediterranean and crossing the northern Adriatic on their way to the northeast, a few episodes were linked to atypical cyclone tracks or, in some cases, not to cyclones at all but to large-scale pressure patterns.

- A review of newspapers and online sources showed that these episodes affected the entire coastline, particularly the northern and middle Adriatic. They continue to disrupt daily life along the coast, sometimes for several days, and in rare cases they result in evacuations, injuries, or even fatalities.

Appendix A
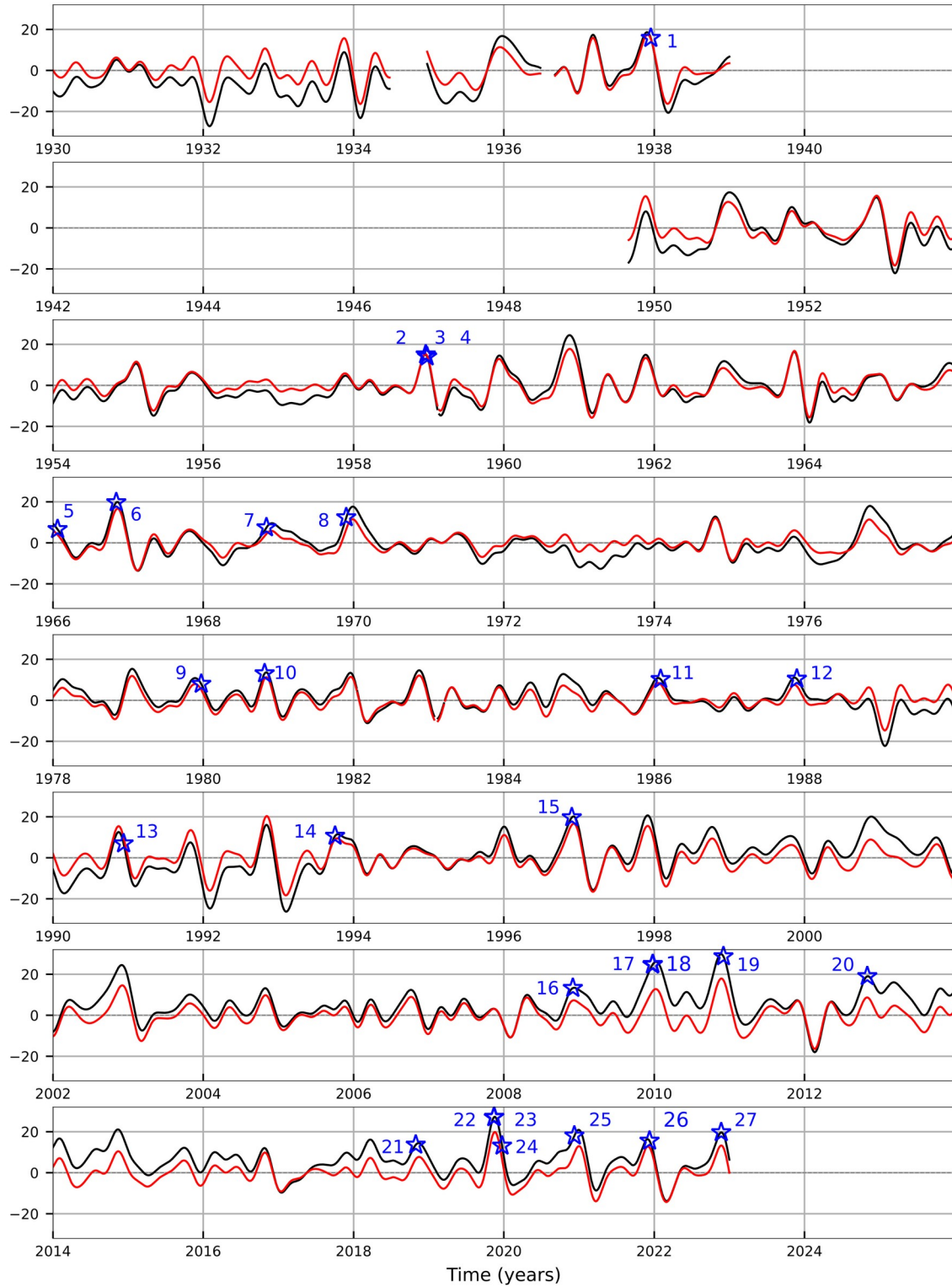
Figure A1: *Long-term sea-level variability* (black; cm), representing SL changes at periods longer than 100 d. Intraannual variability (red), which includes mean seasonal cycle and its anomalies, obtained by high-pass filtering of *long-term sea-level component* at a 15-m cutoff. Blue stars mark the extracted extreme episodes labelled by their IDs from Table 2.